



DR JASON GUY TAYLOR (Orcid ID : 0000-0001-6844-6736)

Article type : Research Article

Design, Synthesis, Molecular Modelling and *In Vitro* Evaluation of Tricyclic Coumarins Against *Trypanosoma Cruzi*

Gleicekelly Silva Coelho^a, Josimara Souza Andrade^a, Viviane Flores Xavier^c, Policarpo Ademar Sales Junior^b, Barbara Caroline Rodrigues de Araujo^a, Kátia da Silva Fonseca^c, Melissa Soares Caetano^a, Silvane Maria Fonseca Murta^b, Paula Melo de Abreu Vieira^c, Claudia Martins Carneiro^c and Jason Guy Taylor^{a*}

^a Chemistry Department, ICEB, Federal University of Ouro Preto, Campus Universitário Morro do Cruzeiro, 35400-000, Ouro Preto-MG, Brazil.

^b René Rachou Institute, FIOCRUZ, 30190-002, Belo Horizonte-MG, Brazil.

^c Immunopathology Laboratory, NUPEB, Federal University of Ouro Preto, Campus Universitário Morro do Cruzeiro, 35400-000, Ouro Preto-MG, Brazil.

* e-mail address of the corresponding author: jason@iceb.ufop.br

Abstract

Chagas disease is caused by infection with the parasite protozoan *Trypanosoma cruzi* and affects about 8 million people in 21 countries in Latin America. The main form of treatment of this disease are still based on the use of two drugs, benznidazole and nifurtimox, which both present low cure rates in the chronic phase and often have serious side effects. Herein, we describe the synthesis of tricyclic coumarins that were obtained via NHC organocatalysis and evaluation of their trypanocidal activity. Molecular docking studies against trypanosomal enzyme triosephosphate isomerase (TIM) were carried out, as well as a theoretical study of the physicochemical parameters. The tricyclic coumarins were tested to *in vitro* against the intracellular forms of *Trypanosoma cruzi*. Amongst the 18 compounds tested, 10 were more active than the reference drug benznidazole. The trypanocidal activity of the lead compound was rationalized by molecular docking study which suggested strong interaction with the enzyme TIM by *T. cruzi* and therefore indicating a possible mode of

This article has been accepted for publication and undergone full peer review but has not been through the copyediting, typesetting, pagination and proofreading process, which may lead to differences between this version and the Version of Record. Please cite this article as doi: 10.1111/cbdd.13420

This article is protected by copyright. All rights reserved.

action. Furthermore, the selectivity index of 8 tricyclic coumarins with high anti *T.cruzi* activity was above 50 and thus showing that these lead compounds are viable candidates for further *in vivo* assays.

Keywords: Chagas disease; coumarins; *Trypanosoma cruzi*; triosephosphate isomerase; isocoumarins; organocatalysis; tricyclic, *in silico*; *in vitro*.

1 Introduction

Neglected Tropical Diseases comprise a group of 17 different types of infections that affect people living on low incomes in mainly developing countries, causing both economic and health problems in patients and their communities. Chagas disease, discovered in 1909 by the Brazilian sanitary doctor Carlos Ribeiro Justiniano Chagas, also called American trypanosomiasis, is an infectious disease caused by the protozoan parasite *Trypanosoma cruzi* (*T. cruzi*) (family Trypanosomatidae, order Kinetoplastida), through direct contact with contaminated feces and/or urine of insects known as barbers (family Reduviidae, subfamily Triatominae).^[1,2] Recently, it was estimated that 6 to 7 million people are infected with Chagas disease worldwide, mostly in Latin America, where it is endemic.^[3,4] Human infection also occurs in nonendemic areas because of growing international immigration and nonvectorial transmission routes such as blood transfusion, organ transplantation, and congenital infection.^[5] *T. cruzi* has four developmental stages: the replicative epimastigote and amastigote stages and the infective non-replicative metacyclic and bloodstream trypomastigote stages.^[1] Chagas disease is characterized by for two phases: acute and chronic. The infection can lead to death due to cardiac arrhythmias or progressive heart failure caused by the destruction of the heart muscle and nervous system.^[1,2] Currently, only two medicines are approved for the treatment of Chagas disease: nifurtimox (NFX) or benznidazole (BZ), both of which were released for sale in the early 1970s.^[6] Both NFX and BZ cause undesirable side effects and present low cure rates mainly in the chronic phase of disease.^[7] Although BZ and NFX drugs can reach a 76% cure rate in acute cases of Chagas disease, their efficiency is dramatic lower in chronic infections where the percentage of cure is around 8%.^[6,7]

Given the negative economic and social impact caused by Chagas disease, lack of vaccines, the limitations of benzimidazoles efficacy in the chronic phase and the existence of naturally resistant *T. cruzi* strains, the search for new drugs has become increasingly necessary to treat this disease. Coumarins (1,2-benzopyrone or benzopiran-2-one), are heterocyclic compounds presents in many plants (*Angiospermas*, *Apiaceae*, *Rutaceae*, *Asteraceae*),^[8] fungi (*Agaricus sp*, *Armillariella tabescens*, *Penicillium*)^[9] and bacteria (*Streptomyces spheroides*, *Streptomyces niveus*).^[10] The isocoumarins are structurally similar to coumarins, differing only by the orientation of the lactone. Reyes-Chilpa *et al.* isolated trypanocidal coumarins from the leaves and bark of *Calophyllum brasiliense* and *Mammea americana* (*Clusiaceae*), both found in America (Figure 1). In 2013, Lago *et al.* isolated and elucidated the antichagasic coumarin soulamarin (Figure 1) from the bark and stem of *Calophyllum brasiliense* (*Clusiaceae*).^[11]

Peacock *et al.* isolated the coumarin chalepine (Figure 2) from *Pilocarpus spicatus* and elucidated the mode of binding of the molecule with the *T. cruzi* enzyme GAPDH which is important for disrupting the glycolytic pathway.^[12] In the search of molecules that can serve as leads in the design of a new drug for the treatment of Chagas' disease, our attention was drawn to brevifolin carboxylate derivatives (Figure 1) isolated from *Geranium bellum* Rose. These compounds were able to inactivate triosephosphate isomerase from *T. cruzi* (TcTIM) in a species-specific manner.^[13] In view of the spectrum of biological activity of naturally occurring coumarins (isolated from plants, fungi and animals), several research groups have searched for new semi-synthetic or synthetic coumarins that contain a spectrum of biological activity better than the natural analogue (Figure 2).

For example, Munoz *et al.*, described the syntheses of 3-carboxyamidocoumarins and evaluation *in vitro* of antitrypanosomal activity these compounds against epimastigotes and trypomastigotes of *T. cruzi*.^[14] In the same year, Vazquez-Rodriguez *et al.* described the synthesis of new coumarin-chalcone hybrids and the evaluated their antitrypanosomal activity against epimastigotes, trypomastigotes and amastigotes of *T. cruzi*.^[15] Ryan *et al.* recently described the synthesis of hydroxyl substituted 3-aryl coumarins and evaluated the antichagasic profile of these compounds against the epimastigote form.^[16] In order to meet this deficit in new drug candidates for Chagas disease, we have prepared and tested 18 tricyclic coumarins against *T. cruzi*, evaluated their cytotoxic effect against L929 cells and determined the selectivity index.

2 Results and Discussion

2.1 Synthesis of tricyclic coumarins

Brevifolin carboxylate derivatives are substituted [6,6,5] tricyclic compounds consisting of an isocoumarin fused to a pentanone ring. Although these compounds were not evaluated for their trypanocidal activity, they were shown to be highly selective inhibitors of triosephosphate isomerase from *T. cruzi* (TcTIM). These preliminary results inspired us to study structurally related compounds in order to uncover more potent molecules against *T. cruzi*. To this end, we synthesised [6,6,5] tricyclic coumarins in order to explore structure activity relationships with TcTIM and determine if inactivation of this enzyme indeed translates into anti *T. cruzi* activity. The synthetic design considered substitution at the phenyl rings or the introduction of heteroaromatic and organometallic moieties to examine their role and trends in terms of electronic and steric contributions. Synthesis of the target compounds **3** (Scheme 1) began with preparation of α,β -unsaturated aldehydes **1** by the Wittig reaction, which afforded substituted cinnamaldehydes in good yield (37-80%). The requisite chalcones **2** were obtained (44-86%) by cross-aldol condensation between substituted 2-hydroxyacetophenones and aromatic aldehydes. All of the intermediates prepared are known compounds and were confirmed by comparison of their physical and spectroscopic data with those reported in the literature.

Next, cinnamaldehydes were reacted with chalcones by a NHC-organocatalyzed homoenolate annulation reaction to furnish tricyclic coumarins **3a-r** in good to excellent yields as shown in scheme 1. Using X-ray diffraction techniques, the relative stereochemistry of the products formed by this reaction had been shown by Biju *et al.* to be predominantly *trans* (*trans* diastereoisomer). In total, 18 coumarins were obtained of which, 15 are novel compounds that were not previously described in the literature. In the case of coumarin **3r**, a hydrogenolysis of **3q** was carried out in the presence of ammonium formate and palladium (Pd/C 5%) to cleave the benzyl group and liberate the free hydroxyl. Compounds **3a-r** were characterized by FT-IR, HRMS and ^1H and ^{13}C nuclear magnetic resonance spectroscopy. In the infrared spectrum, the carbonyl group displays a distinctive band at approximately 1716 cm^{-1} corresponding to the lactone carbonyl group. In the ^1H NMR spectrum, all tricyclic coumarins exhibited a characteristic double doublet resonance corresponding to a methylene hydrogen ($\delta = 3.32$ ppm) and a doublet resonance corresponding to a methine hydrogen ($\delta = 4.41$ ppm) located at the same position as the R2 substituent. The key ^{13}C NMR signals

include the carbonyl carbon ($\delta = 158.6$ ppm) and 3 other signals corresponding to sp^3 carbons that form part of the cyclopentene moiety ($\delta = 53.4, 59.1$ and 39.5 ppm). The molecular formula assignment was further supported by HRMS data and GC-MS was also carried out to evaluate product purity. It has been well documented that for pharmacological active racemic mixtures, one enantiomer is mainly responsible for the desired biological action (eutomer) and the other inactive (distomer). Although the enantioselective version of the NHC-catalyzed reaction between enals and hydroxy chalcones had not yet been reported, an attempt at the asymmetric reaction was carried out in the hope of obtaining an enantiomerically pure sample for biological testing. The chiral triazol **4** has successfully been applied to the asymmetric synthesis of cyclopentanones^[17,18] and the asymmetric intramolecular Stetter reaction.^[19,20] Compound **4** (Figure 3) was therefore employed as catalyst (10 mol%) for the homoenolate annulation reaction but unfortunately, no reaction occurred and only the starting materials were recovered.

Nevertheless, with the racemic compounds in hand, *in vitro* bioassays using trypanomastigote and amastigote forms of Y-strain *T. cruzi* were carried out.

2.2 Molecular docking in Human Triosephosphate isomerase (4POC) enzyme and *T. cruzi* Triosephosphate isomerase enzyme (1TOC).

Computational simulation and molecular docking studies are an important research technique for evaluating molecular interactions between the protein and the ligand, since the 3D structure of the protein has been elucidated. Through molecular docking it is possible to predict the most stable structure of the protein-ligand complex, and also to calculate the energy of interaction^[21] based on preliminary study of Gayosso-De-Lucio *et. al.*,^[13] that described the inactivation of the *T. cruzi* triosephosphate isomerase (TIM) enzyme by isocoumarins isolated from *hellum rose geranium*, this study was performed with molecular docking in silico of new coumarin compounds. The objective was to investigate the enzyme-compound interaction and thus predict which groups are responsible for the interaction with the enzyme and determine the key amino acid residues participate in this interaction.

Three-dimensional structures of human and tripanossomal triosephosphate isomerase (TIM) enzymes were obtained from "Protein Data Bank" (PDB) with the 4POC and 1TCD codes, respectively. With the Molegro Virtual Docker software (MVD), molecular docking calculation of the compounds were carried out in both TIM enzymes in order to identify the mode of the ligand interactions by estimating the number of solutions and the power associated with its interactions with the protein. The binding sites between the coumarins and TIM enzymes were determined by a prediction algorithm based on a 3D box, through the MVD software. The volume of the cavity is 35.33 Å³ (TIM human) and 37,38 Å³ (TIM *T. cruzi*). The interaction energy values and hydrogen bonds were calculated for the enzyme-compound complex, and verified which groups are responsible for activity. Table 1 contains the amino acids that participate in the enzyme - compound interaction and the energy interaction values.

Notably, compound **3p** containing a styryl substituent interacted more strongly (-143.12 kcal mol⁻¹) with *T. cruzi* TIM enzyme than any other tricyclic coumarin as indicated by having the lowest energy value of compounds **3a-r**. Although the compound in question does not perform hydrogen bonding interactions with the amino acid residues of the active site of the enzyme, it stabilizes, as well as other compounds, performing π stacking interactions with Tyr103 residue that appears to be of great importance for a good ligand-enzyme interaction (Figure 4).

The second best result was observed for compound **3e** containing a *p*-methoxyphenyl group. The interaction energy was calculated to be -139.35 kcal mol⁻¹ and the existence of a hydrogen bond between the methoxy group and the amino acid residue Arg99 was observed (Figure 5).

Compound **3e** in spite of having hydrogen interactions behaved similarly to **3p** in that they both share a common π stacking type interaction with amino acid residue Tyr103. These two compounds are best stabilized in the active site of *T. cruzi* TIM enzyme adopted very similar conformations, which can be seen in the following overlapping figure (Figure 6).

Interestingly, the compounds **3j**, **3k** and **3m** containing heterocyclic groups did not show good interactions with the human TIM enzyme which indicated potentially low toxicity for these coumarins. It is further noted that the compounds **3j** and **3n**, containing either a furan or pyridine moiety presented good interaction with the *T. cruzi* TIM enzyme which suggests these coumarins could be more selective. Observing the behaviour of the coumarins in the active site of *T. cruzi* TIM, it was possible to observe that the compounds **3m** and **3k** do not perform intermolecular π stacking interactions with amino acid residues Tyr 103 but perform intramolecular π stacking interaction that do not favour its stabilization in the enzyme (Figure 7).

Interestingly, compound **3n** containing two pyridine rings showed lowest stability in the active site of human TIM enzyme ($-30.75 \text{ kcal mol}^{-1}$) amongst the evaluated compounds. Given this large difference in interaction energy presented by compound **3n** in relation to human and tripanossomal enzymes, this compound stands out as a potential ligand since it is expected to be highly selective. Coumarin **3r** interacts with *T. cruzi* TIM enzyme by hydrogen bonding between the free hydroxyl group and amino acids residues Arg99 and Glu78, indicating that the presence of hydroxyl help stabilize the compound in the active site of the enzyme (Figure 8). Moreover, **3r** also showed good interaction with the human TIM enzyme, a difference of $3.44 \text{ kcal mol}^{-1}$. This ligand adopts at the binding site a conformation in which its non-fused aromatic rings are on opposite sides not performing intramolecular π stacking interaction but intermolecular π stacking interaction once again with the amino acid residue Tyr103.

2.3 Evaluation of *in vitro* anti *T. cruzi* activity

Once the final products were purified and fully characterized we carried out *in vitro* bioassays against trypomastigote and intracellular amastigote of β -galactosidase transfected Tulahuen strain of *T. cruzi*. There have been different approaches taken towards the *in vitro* evaluation of anti *T. cruzi* activity. The use of the epimastigote form present in the midgut vector can be employed for an *in vitro* screening method,^[21,22] but we have opted for a methodology that simultaneously evaluates trypomastigote forms that are initially present in the blood after entering through the bite wound and intracellular amastigotes forms present in the vertebrate host during the acute and chronic phases of the disease.^[23,24] This approach is in accordance

with the guidelines proposed by the Fiocruz Program for Research and Technological Development on Chagas Disease and the Drugs for Neglected Diseases Initiative (DNDi).^[23,24] Furthermore, the whole cell-based screening methodology is also attractive given that bioactive compounds can be tested for anti *T. cruzi* activity in infected cells whilst at the same time monitoring their effects on both amastigotes and trypomastigotes in the same system. Benznidazole was used as positive control against *T. cruzi* and cytotoxicity was determined in mammalian L929 cells (Table 2). Amongst the 18 compounds tested, ten of these were more active than reference drug benznidazole and eight had selectivity indexes above 50. In all cases, the tested compounds were more toxic and less selective than reference compound benznidazole. Nevertheless, following the guidelines suggested by Fiocruz and DNDi,^[25] compounds with a selectivity index equal to or greater than 50 are highly selective and are recommended for *in vivo* testing. Therefore, 8 of the 18 tricyclic coumarins tested would be suitable lead compounds for *in vivo* testing. Initially, compound **3a** was evaluated for trypanocidal activity and this result used for comparison in order to assess structure activity relationships. The IC₅₀ for **3a** (2.5 μM) was slightly better than the reference compound and this initial preliminary result encouraged us to investigate other analogues bearing substituents capable of forming stronger intermolecular interactions with the TcTim which is our intended target for bioactivity. The most selective compound was coumarin **3e** (SI = 262) which differs from **3a** (SI = 128) by containing an anisole substituent instead of a benzene at the R1 position of the cyclopentene portion of the molecule. Similarly, compound **3l**, which also bears an anisole substituent on the cyclopentene ring but in this case at the R2 position, demonstrated almost identical anti *T. cruzi* activity to **3e** but with significantly greater cytotoxicity and ultimately lower selectivity. The improvement in *T. cruzi* activity observed for coumarins bearing a methoxy group suggests some important hydrogen bonding interaction with TcTIM. The importance of methoxy substituents was also noted for the trypanocidal activity of coumarin-chalcone hybrid molecules.^[13] The chlorobenzene group present in **3g** resulted in compound that was equipotent to benznidazole but four times more toxic than **3a** thus making the presence of a chloro atom undesirable. Compound **3p** which contains a styryl group at the R1 position, was the most potent coumarin tested against *T. cruzi*, with IC₅₀ value of 0.46 ± 0.12 μM and selectivity index SI = 83.7. This trypanocidal activity represents an increase in potency of 6 fold in comparison with **3a** and **3p** is also approximately 10 times more potent than benznidazole. According to the molecular docking study, this compound presented one of the best molecular interaction energies with TcTim (-143.12 kcal mol⁻¹) and therefore may explain the trend in structure

activity relationships that occurred during *in vitro* testing. Some promising biological activities of ferrocenes against *T.cruzi* have been reported in the literature ^[26,27] and this motivated us to synthesis and test an analogous compound **3o** in this study. The presence of a ferrocene did not significantly improve either trypanocidal activity or selectivity when compared to **3a** but the *in vitro* results for this compound were still promising and it should be noted that cytotoxicity was reasonably low *in vitro*. Our lead compounds **3e** and **3p** were subjected to *in vitro* bioassays using the epimastigote form present in the midgut vector and presented IC₅₀ values of 103μM and 109 μM respectively. Surprisingly, the impressive typanocidal activities observed against amastigotes and trypomastigotes were not replicated against epimastigotes. Several studies have demonstrated a higher resistance of the *T. cruzi* epimastigote form to drugs, when compared to amastigote and trypomastigote forms ^[28,29] and it should be emphasized that amastigotes and trypomastigotes are the relevant forms to human infection. The potential of compounds **3a-r** as candidates for new drugs was also evaluated by using Linpinski parameters, which considers the physicochemical drug descriptors of the molecular properties for the synthesized compounds as calculated by Molinspiration software. The partition coefficient (LogP: octanol/water partition coefficient) describes the equilibrium distribution between two liquid phases such as octanol and water and the total polar surface area (TPSA) is a measure of the extent of the molecules exposed polar area. The risk of toxicity related to mutagenic and tumorigenic effects were determined by utilizing "OSIRIS property explorer". The results show that compounds **3j-k** and **3m-o** satisfy Linpinski's rule of five with no violations.^[30] The other compounds violate the rule by presenting lipophilicity (Log P) greater than 5.0, which could cause problems with oral bioavailability. All compounds showed TPSA values lower than 90 Å², values obtained range from 30-60 Å², indicating that these compounds would have a good permeability in the plasma cell membrane and across the blood brain barrier. The risk of theoretical toxicity was estimated by the OSIRIS program and this program classifies the risks of toxicity as either high risk (HR), medium risk (MR), low risk (LR) or no risk (NR). Assessment of the toxicity revealed that none of the compounds presented potential irritant effects. Only compound **3o** containing the ferrocene group presented high risk for mutagenic effect and low risk for tumorigenic effect and all other coumarins did not present any of these risks.

3 Conclusion

The NHC organocatalysis strategy was applied to the synthesis of 18 tricyclic coumarins, of which 15 are novel compounds. All compounds satisfy the Lipinski rule parameters, and theoretically, all have adequate oral availability. Molecular modeling studies showed that the compounds are stabilized at the active site of the TcTIM *T. cruzi* enzyme by intermolecular interactions and in particular, the presence of a styryl substituent showed strongest interaction with TcTIM. The anti *T. cruzi* activity of 18 tricyclic coumarins were evaluated *in vitro* against amastigote and tripomastigote forms of parasite. Most of the evaluated coumarins presented promising activity against the intracellular forms of *T. cruzi*, with ten compounds presenting IC₅₀ values lower than the benznidazole. Regarding the selectivity index, a criterion analyzed for the screening of possible drugs for subsequent *in vivo* tests, eight compounds are suitable for *in vivo* assays. Further studies to determine experimentally the mechanism of action of the tricyclic coumarins and *in vivo* evaluation of our lead compounds are ongoing.

4 Experimental Section

All commercial reagents were used as received. Anhydrous solvents were purchased from Sigma Aldrich. Flash column chromatography was performed using silica gel 200-400 Mesh. TLC analyses were performed using silica gel plates, using ultraviolet light (254 nm), phosphomolybdic acid or vanillin solution for visualization. Melting points are uncorrected and were recorded on a Buchi B-540 apparatus. For NMR data, the chemical shifts are reported in δ (ppm) referenced to residual solvent protons and ¹³C signals in deuterated chloroform. Coupling constants (*J*) are expressed in Hertz (*Hz*). Infrared spectra were obtained on a Thermo Scientific Nicolet 380 FT-IR apparatus (600–4000 cm⁻¹, Nicolet Instrument Corp., Madison, WI, USA) using attenuated total reflection (ATR). Mass spectra were obtained by GC-MS, Shimadzu QP-2010 Plus model (Shimadzu, Kyoto, Japan) and High Resolution Mass Spectra were obtained on a Shimadzu HPLC-ESI-IT-TOF. SMILES notations of the tricyclic coumarins derivatives were inputted into an online software and subjected to molecular properties prediction by Molinspiration software (software version v2015.01).

4.1 Typical procedure for synthesis of tricyclic coumarins 3a-r: Chalcone (1 mmol), cinnamaldehyde (1 mmol), 1,3-Bis(2,4,6-trimethylphenyl)imidazolium chloride (10 mol%), were added to the Schlenk tube and the atmosphere was purged with nitrogen. Thereafter, 1,8-diazabicyclo[5.4.0]undec-7-ene (20 mol%) and anhydrous tetrahydrofuran (4 mL) were added with the aid of a syringe and the reaction mixture being kept under stirring for 12 hours at room temperature. The solvent was evaporated with the aid of rotary evaporator and the crude mixture was purified by flash column chromatography on silica gel, eluting with ethyl acetate and hexane.

trans-2,3-diphenyl-2,3-dihydrocyclopenta[*c*]chromen-4(*1H*)-one (**3a**): Product obtained as a white solid in 49%, mp. 124-126°C; R_f: 0.2 (ethyl acetate/hexane 2:8); IR (cm⁻¹): 3026, 2941, 1718, 1618, 1452, 1274, 1043, 761, 700; ¹H-NMR (400 MHz, CDCl₃): δ 3.33 (dd, *J* 8.0 Hz, *J* 20.0 Hz, 1H), 3.82 (m, 2H), 4.52 (d, *J* 4 Hz, 1H), 7.61 (m, 14H); ¹³C-NMR (75 MHz, CDCl₃): δ 39.5, 53.4, 59.1, 116.9, 118.3, 124.2, 125.0, 126.8, 126.9, 127.0, 128.6, 128.7, 128.8, 131.4, 142.3, 144.5, 154.7, 155.5, 158.8. EI *m/z*: 260 (100%), 247 (50%), 203 (70%), 189 (30%), 130 (20%), 91 (40%); HRMS (ESI-TOF) *m/z* [M + Na]⁺ Calcd for C₂₄H₁₈NaO₂: 361.1199; Found: 361.1186.

trans-3-(2-chlorophenyl)-2-phenyl-2,3-dihydrocyclopenta[*c*]chromen-4(*1H*)-one (**3b**): Product obtained as a pale yellow oil in 74%; R_f: 0.58 (ethyl acetate/hexane 2:8); IR (cm⁻¹): 3024, 2921, 1720, 1606, 1452, 1216, 1039, 746, 696; ¹H-NMR (300 MHz, CDCl₃): δ 3.30 (dd, *J* 9.0 Hz, *J* 21.0 Hz, 1H), 3.74 (m, 1H), 5.00 (d, *J* 3.0 Hz, 1H), 7.61 (m, 14H); ¹³C-NMR (75 MHz, CDCl₃): δ 39.3, 52.2, 55.4, 117.0, 118.2, 124.3, 125.0, 126.8, 127.0, 127.9, 128.1, 128.7, 130.1, 131.6, 133.9, 139.3, 144.4, 154.8, 156.5, 158.6; EI *m/z*: 372 (5%), 337 (100%), 259 (10%), 202 (10%), 144 (10%), 91 (20%); HRMS (ESI-TOF) *m/z* [M + H]⁺ calcd for C₂₄H₁₈ClO₂: 373.0990; Found: 373.0962.

trans-3-(3-methoxyphenyl)-2-phenyl-2,3-dihydrocyclopenta[*c*]chromen-4(*1H*)-one (**3c**): Product obtained as a pale yellow solid in 76%, mp. 146-148°C; R_f: 0.2 (ethyl acetate/hexane 1:9); IR (cm⁻¹): 2943, 1730, 1608, 1452, 1384, 1272, 1043, 756, 698; ¹H-NMR (300 MHz, CDCl₃): δ 3.29 (dd, *J* 6 Hz, *J* 18 Hz, 1H), 3.79 (m, 5H), 4.47 (d, *J* 6 Hz, 1H), 7.60 (m, 13H); ¹³C-NMR (75 MHz, CDCl₃): δ 39.4, 53.2, 55.1, 59.1, 115.1, 113.1, 116.9, 118.3, 119.4, 124.2, 125.0, 126.7, 126.9, 128.5, 128.8, 129.7, 131.5, 144.0, 144.6, 154.7, 155.6, 158.8, 159.7; EM *m/z*: 368 (100%), 353 (10%), 337 (5%), 260 (80%), 218 (30%), 145 (20%), 91

(40%); HRMS (ESI-TOF) m/z $[M+Na]^+$ calcd for $C_{25}H_{20}NaO_3$: 391.1305; Found: 391.1274.

trans-3-(3-bromophenyl)-2-phenyl-2,3-dihydrocyclopenta[*c*]chromen-4(1*H*)-one (3d):

Product obtained as a pale yellow oil in 80%; R_f : 0.3 (ethyl acetate/hexane 1:9); IR (cm^{-1}): 2914, 1716, 1608, 1454, 1390, 1068, 1216, 1043, 756, 698, 684; 1H -NMR (300 MHz, $CDCl_3$): δ 3.32 (dd, J 6 Hz, J 18 Hz, 1H), 3.58 (m, 2H), 4.45 (d, J 6 Hz, 1H), 7.60 (m, 13H); ^{13}C -NMR (75 MHz, $CDCl_3$): δ 39.5, 53.4, 58.8, 117.0, 118.1, 122.8, 124.3, 125.1, 126.0, 126.8, 127.8, 128.9, 130.1, 130.2, 131.7, 143.9, 144.7, 154.8, 155.9, 158.6; EM m/z : 417 (60%), 337 (80%), 260 (40%), 246 (50%), 202 (50%), 189 (20%), 91 (100%); HRMS (ESI-TOF) m/z $[M+H]^+$ calcd for $C_{24}H_{18}BrO_2$: 417.0485; Found: 417.0468.

trans-2-(4-methoxyphenyl)-3-phenyl-2,3-dihydrocyclopenta[*c*]chromen-4(1*H*)-one (3e):

Product obtained as a white solid in 65%; R_f : 0.5 (ethyl acetate/hexane 2:8); IR (cm^{-1}): 3024, 1722, 1606, 1452, 1384, 1178, 1249, 1033, 750, 680; 1H -NMR (300 MHz, $CDCl_3$): δ 3.27 (dd, J 6 Hz, J 18 Hz, 1H), 3.77 (m, 2H), 3.80 (s, 3H), 4.46 (d, J 6 Hz, 1H), 7.59 (m, 13H); ^{13}C -NMR (75 MHz, $CDCl_3$): δ 39.5, 52.8, 55.2, 59.3, 114.2, 116.9, 118.4, 124.2, 125.0, 126.8, 127.0, 127.8, 128.6, 131.4, 136.5, 142.4, 154.8, 155.5, 158.5, 158.6; EM m/z : 368 (90%), 353 (5%), 337 (5%), 260 (100%), 207 (40%), 121 (40%), 91 (20%); HRMS (ESI-TOF) m/z $[M+H]^+$ calcd for $C_{25}H_{21}O_3$: 369.1485; Found: 369.1478.

trans-2-(4-fluorophenyl)-3-phenyl-2,3-dihydrocyclopenta[*c*]chromen-4-(1*H*)-one (3f):

Product obtained as a white solid in 43%, mp: 1135-137°C; R_f : 0.5 (ethyl acetate/hexane 1:9); IR (cm^{-1}): 3064, 1724, 1604, 1452, 1390, 1226, 1037, 754, 700; 1H -NMR (300 MHz, $CDCl_3$): δ 3.27 (dd, J 6 Hz, J 18 Hz, 1H), 3.80 (m, 2H), 4.44 (d, J 3 Hz, 1H), 7.60 (m, 13H); ^{13}C -NMR (75 MHz, $CDCl_3$): δ 39.5, 52.8, 115.8-115.3 (d, J_{C-F} 21.0 Hz), 117.0, 118.2, 124.3, 125.0, 127.0, 128.4 – 128.3 (d, J_{C-F} 7.5 Hz), 128.4, 128.7, 140.1 – 140.0 (d, J_{C-F} 3 Hz); 142.1, 154.7, 155.3, 158.7, 163.3 – 160.1 (d, J_{C-F} 243.7 Hz); EM m/z : 356 (100%), 278 (30%), 260 (70%), 220 (10%), 203 (40%), 91 (20%). HRMS (ESI-TOF) m/z $[M+H]^+$ calcd for $C_{24}H_{18}FO_2$: 357.1285; Found: 357.1258.

trans-8-chloro-2,3-diphenyl-2,3-dihydrocyclopenta[*c*]chromen-4-(1*H*)-one (3g):

Product obtained as a white solid in 49%, mp: 183-185°C; R_f : 0.6 (ethyl acetate/hexane 2:8); IR (cm^{-1}): 3029, 1720, 1631, 1492, 1263, 1031, 730, 696, 669; 1H -NMR (300 MHz, $CDCl_3$): δ 3.30 (dd, J 9 Hz, J 24 Hz, 1H), 3.77 (m, 2H), 4.50 (d, J 6 Hz, 1H), 7.52 (m, 13H); ^{13}C -NMR (75 MHz, $CDCl_3$): δ 39.3, 53.2, 59.2, 118.3, 119.4, 124.5, 126.7, 127.0, 128.7, 128.9, 129.5,

129.8, 131.3, 142.0, 144.2, 153.1, 154.2, 158.1; EM m/z : 372 (100%), 337 (10%), 294 (80%), 218 (40%), 202 (90%), 91 (40%). HRMS (ESI-TOF) m/z $[M+H]^+$ calcd for $C_{24}H_{18}ClO_2$: 373.0990; Found: 373.0993.

trans-8-chloro-3-(4-chlorophenyl)-2-phenyl-2,3-dihydrocyclopenta[*c*]chromen-4-(1*H*)-one

(3h): Product obtained as a beige solid in 68%, mp: 218-220°C; R_f : 0.7 (ethyl acetate/hexane 2:8); IR (cm^{-1}): 3066, 1728, 1604, 1488, 1257, 1022, 765, 727, 696; 1H -NMR (300 MHz, $CDCl_3$): δ 3.28 (dd, J 3 Hz, J 15 Hz, 1H), 3.74 (m, 2H), 4.45 (d, J 3 Hz, 1H), 7.53 (m, 13H); ^{13}C -NMR (75 MHz, $CDCl_3$): δ 39.3, 53.5, 59.6, 118.3, 119.3, 124.5, 126.8, 127.2, 128.4, 128.9, 128.9, 129.0, 129.2, 129.6, 131.5, 140.3, 143.4, 153.1, 154.5, 158.0; EM m/z : 406 (20%), 371 (20%), 294 (10%), 281 (20%), 207 (100%), 91 (15%). HRMS (ESI-TOF) m/z $[M+Na]^+$ calcd for $C_{24}H_{16}Cl_2NaO_2$: 429.0424; Found: 429.0425.

trans-8-chloro-3-(4-methoxyphenyl)-2-phenyl-2,3-dihydrocyclopenta[*c*]chromen-4-(1*H*)-one

(3i) Product obtained as a white solid in 85%, mp: 103-105°C; R_f : 0.6 (ethyl acetate/hexane 2:8); IR (cm^{-1}): 2925, 1724, 1612, 1510, 1377, 1174, 1245, 1027, 821, 765, 702; 1H -NMR (300 MHz, $CDCl_3$): δ 3.25 (dd, J 3 Hz, J 15 Hz, 1H), 3.74 (m, 2H), 3.78 (s, 3H), 4.44 (d, J 3 Hz, 1H), 7.51 (m, 12H); ^{13}C -NMR (75 MHz, $CDCl_3$): δ 39.3, 53.4, 55.2, 58.4, 114.1, 118.3, 119.5, 124.5, 126.7, 126.9, 128.0, 128.8, 129.5, 130.0, 131.2, 134.1, 144.1, 153.1, 153.9, 158.1, 158.6; EM m/z : 402 (100%), 387 (5%), 371 (5%), 324 (40%), 294 (80%), 266 (30%), 232 (20%), 207 (15%), 162 (20%), 91 (20%). HRMS (ESI-TOF) m/z $[M+H]^+$ calcd for $C_{25}H_{20}ClO_3$: 403.1101; Found: 403.1109.

trans-2-(furan-2-yl)-8-methoxy-3-phenyl-2,3-dihydrocyclopenta[*c*]chromen-4(1*H*)-one **(3j)**:

Product obtained as a yellow oil in 67%; R_f : 0.6 (ethyl acetate/hexane 2:8); IR (cm^{-1}): 2923, 1720, 1573, 1494, 1272, 1074, 1199, 1012, 738, 702; 1H -NMR (300 MHz, $CDCl_3$): δ 3.36 (dd, J 3 Hz, J 15 Hz, 1H), 3.77 (m, 2H), 3.88 (s, 3H), 4.61 (d, J 6 Hz, 1H), 6.10 (d, J 3 Hz, 1H), 6.31 (d, J 3 Hz, 1H), 6.96 (d, J 3 Hz, 1H), 7.37 (m, 8H); ^{13}C -NMR (75 MHz, $CDCl_3$): δ 29.6, 36.5, 46.5, 55.8, 105.1, 107.51, 110.2, 117.9, 118.7, 118.7, 127.0, 127.1, 128.7, 141.8, 149.1, 154.6, 156.0, 156.1, 158.8; EM m/z : 358 (100%), 329 (50%), 290 (30%), 262 (20%), 67 (5%), 55 (15%). HRMS (ESI-TOF) m/z $[M+Na]^+$ calcd for $C_{23}H_{18}NaO_4$: 381.1097; Found: 381.1062.

trans-2-(1-methyl-1*H*-pyrrol-2-yl)-3-phenyl-2,3-dihydrocyclo-penta[*c*]chromen-4(1*H*)-one (**3k**): Product obtained as a yellow oil in 36%; R_f : 0.7 (ethyl acetate/hexane 3:7); IR (cm^{-1}): 3425, 2916, 1722, 1631, 1454, 1386, 1043, 775, 694; $^1\text{H-NMR}$ (300 MHz, CDCl_3): δ 3.35 (m, 4H), 3.75 (m, 2H), 4.47 (d, J 6 Hz, 1H), 6.57 (m, 3H), 7.57 (m, 9H); $^{13}\text{C-NMR}$ (75 MHz, CDCl_3): δ 33.9, 38.1, 44.8, 58.0, 104.6, 106.9, 116.9, 118.3, 122.3, 124.2, 124.9, 127.2, 128.4, 128.8, 131.4, 135.2, 142.0, 154.7, 154.9, 158.8; EM m/z : 341 (80%), 264 (5%), 260 (80%), 165 (50%), 94 (40%), 81 (100%), 77 (20%); HRMS (ESI-TOF) m/z $[\text{M}+\text{H}]^+$ calcd for $\text{C}_{23}\text{H}_{20}\text{NO}_2$: 342.489; Found: 342.1469.

trans-2-(2-chlorophenyl)-3-(4-methoxyphenyl)-2,3-dihydrocyclo-penta[*c*]chromen-4-(1*H*)-one (**3l**): Product obtained as a yellow oil in 89%; R_f : 0.3 (ethyl acetate/hexane 1:9); IR (cm^{-1}): 2918, 1722, 1608, 1450, 1245, 1035, 1176, 1107, 831, 750, 678; $^1\text{H-NMR}$ (300 MHz, CDCl_3): δ 3.25 (dd, J 6 Hz, J 21 Hz, 1H), 3.83 (m, 4H), 4.15 (m, 3H), 4.57 (d, J 6 Hz, 1H), 7.58 (m, 12H); $^{13}\text{C-NMR}$ (75 MHz, CDCl_3): δ 38.2, 49.4, 55.0, 56.4, 114.1, 116.9, 118.4, 124.5, 125.0, 127.3, 127.6, 128.0, 128.1, 128.2, 129.0, 129.9, 131.4, 133.6, 134.1, 141.7, 154.7, 154.9, 158.8; EM m/z : 402 (100%), 387 (5%), 367 (30%), 335 (5%), 290 (40%), 259 (60%), 232 (20%), 145 (40%), 77 (25%); HRMS (ESI-TOF) m/z $[\text{M}+\text{H}]^+$ calcd for $\text{C}_{25}\text{H}_{20}\text{ClO}_3$: 403.1101; Found: 403.1091.

trans-2-(furan-2-yl)-3-phenyl-2,3-dihydrocyclopenta[*c*]chromen-4(1*H*)-one (**3m**): Product obtained as a white solid in 59%, mp: 130-131°C; R_f : 0.46 (ethyl acetate/hexane 3:7); IR (cm^{-1}): 2925, 1720, 1608, 1454, 1390, 1037, 1216, 1012, 750; $^1\text{H-NMR}$ (300 MHz, CDCl_3): δ 3.39 (d, J 3 Hz, J 18 Hz, 1H), 3.70 (m, 2H), 4.61 (d, J 3 Hz, 1H), 6.32 (m, 2H), 7.58 (m, 10H); $^{13}\text{C-NMR}$ (75 MHz, CDCl_3): δ 36.4, 46.6, 55.8, 105.2, 110.2, 116.9, 118.3, 124.2, 124.9, 127.0, 127.1, 128.2, 128.7, 131.4, 141.9, 154.7, 155.1, 156.0, 158.8; EM m/z : 328 (100%), 260 (60%), 126 (10%), 91 (40%); HRMS (ESI-TOF) m/z $[\text{M}+\text{H}]^+$ calcd for $\text{C}_{22}\text{H}_{17}\text{O}_3$: 329.1172; Found: 329.1175.

trans-2,3-di(2-pyridinyl)-2,3-dihydrocyclopenta[*c*]chromen-4(1*H*)-one (**3n**): Product obtained as a white solid in 91%, mp: 135-136°C; R_f : 0.26 (ethyl acetate/hexane 2:8); IR (cm^{-1}): 3008, 1722, 1591, 1434, 1218, 1390, 1037, 752; $^1\text{H-NMR}$ (300 MHz, CDCl_3): δ 3.78 (m, 2H), 4.27 (dd, J 3 Hz, J 6 Hz, 1H), 4.85 (d, J 3 Hz, 1H), 7.08 (d, 1H, J 6 Hz), 7.66 (m, 9H), 8.60 (d, J 3 Hz, 1H), 8.64 (d, J 3 Hz, 1H); $^{13}\text{C-NMR}$ (75 MHz, CDCl_3): δ 37.9, 52.9, 59.3, 116.8, 118.7, 122.0, 122.0, 122.7, 123.8, 124.1, 125.1, 128.0, 131.2, 136.5, 136.6, 149.8,

149.9, 154.7, 155.9, 159.0, 161.0, 162.2; EM m/z : 340 (80%), 262 (100%), 1455 (5%), 78 (70%); HRMS (ESI-TOF) m/z $[M+Na]^+$ calcd for $C_{22}H_{16}N_2NaO_3$: 363.1104; Found: 363.1108.

trans-2-(ferrocenyl)-3-phenyl-2,3-dihydrocyclopenta[*c*]chromen-4(1*H*)-one (**3o**): Product obtained as a yellow solid in 48%, mp: 184-185°C; R_f : 0.32 (ethyl acetate/hexane 1:9); IR (cm^{-1}): 3080, 1724, 1629, 1490, 1388, 1035, 765; 1H -NMR (300 MHz, $CDCl_3$): δ 3.29 (dd, J 3 Hz, J 18 Hz, 1H), 3.74 (m, 2H), 4.14 (m, 9H), 4.40 (d, J 3 Hz, 1H), 7.61 (m, 10H); ^{13}C -NMR (75 MHz, $CDCl_3$): δ 36.4, 46.6, 55.8, 65.8, 67.1, 67.7, 67.8, 68.4, 92.2, 116.9, 118.4, 124.1, 124.9, 126.9, 127.3, 128.7, 129.0, 131.3, 142.6, 154.6, 154.9, 158.8; HRMS (ESI-TOF) m/z $[M+H]^+$ calcd for $C_{28}H_{23}FeO_2$: 447.1042; Found: 447.1041.

trans-3-phenyl-2-(*E*)-styryl-2,3-dihydrocyclopenta[*c*]chromen-4(1*H*)-one (**3p**): Product obtained as a yellow oil in 59%; R_f : 0.44 (ethyl acetate/hexane 2:8); IR (cm^{-1}): 2916; 1718, 1608, 1452, 1384, 1037, 1242, 1029, 742; 1H -NMR (300 MHz, $CDCl_3$): δ 3.10 (dd, J 6 Hz, J 18 Hz, 1H), 3.62 (m, 2H), 4.31 (d, J 3 Hz, 1H), 6.39 (d, J 6 Hz, 1H), 7.57 (m, 15H); ^{13}C -NMR (75 MHz, $CDCl_3$): δ 37.4, 51.7, 56.9, 116.9, 118.4, 124.2, 125.0, 125.5, 126.2, 126.9, 127.2, 128.5, 128.6, 129.8, 130.5, 131.4, 132.4, 136.8, 141.8, 154.6, 155.5, 158.9; EM (m/z): 364 (60%), 273 (40%), 260 (100%), 202 (10%), 180 (40%), 91 (60%); HRMS (ESI-TOF) m/z $[M+Na]^+$ calcd for $C_{26}H_{20}NaO_2$: 387.1356; Found: 387.1360.

trans-2-(4-benzyloxy)phenyl-3-phenyl-2,3-dihydrocyclopenta[*c*]chromen-4(1*H*)-one (**3q**): Product obtained as a yellow oil in 49%; R_f : 0.32 (ethyl acetate/hexane 2:8); IR (cm^{-1}): 2920, 1724, 1608, 1452, 1386, 1178, 1243, 1026, 748; 1H -NMR (300 MHz, $CDCl_3$): δ 3.28 (dd, J 6 Hz, J 18 Hz, 1H), 3.79 (m, 2H), 4.47 (d, J 6 Hz, 1H), 5.07 (s, 2H), 7.58 (m, 18H); ^{13}C -NMR (75 MHz, $CDCl_3$): δ 41.0, 52.8, 59.3, 70.0, 115.1, 116.9, 118.3, 124.2, 125.0, 127.0, 127.5, 127.9, 128.0, 128.6, 128.7, 131.4, 136.8, 136.9, 142.2, 154.7, 155.7, 157.7, 158.8; HRMS (ESI-TOF) m/z $[M+H]^+$ calcd for $C_{31}H_{25}O_3$: 445.1803; Found: 444.1814.

4.2 Typical procedure for synthesis of tricyclic coumarin 3r: To a Schlenk Tube was added compound **3q** (1 mmol), palladium acetate (5 mol%) and Pd/C 5% (1 equiv.). Next, the atmosphere was purged with N_2 . Ammonium formate (15 mmol.) dissolved in methanol was added by syringe and the temperature was raised to 60°C and maintained for 2-3 hours. The mixture was cooled to room temperature, concentrated and the crude mixture purified by flash column chromatography eluting with ethyl acetate and hexane.

trans-2-(4-hydroxyphenyl)-3-phenyl-2,3-dihydrocyclopenta[*c*]chromen-4-(1*H*)-one (3r): Product obtained as a white solid in 26%, mp: 196-197; R_f: 0.5 (ethyl acetate/hexane 1:9); IR (cm⁻¹): 3282, 2925, 1693, 1606, 1454, 1388, 1056, 1224, 763; ¹H-NMR (300 MHz, CDCl₃): δ 3.25 (dd, *J* 6 Hz, *J* 18 Hz, 1H), 3.76 (m, 2H), 4.43 (d, *J* 6 Hz, 1H), 7.56 (m, 13H); ¹³C-NMR (75 MHz, CDCl₃): 39.6, 52.8, 59.3, 115.6, 117.0, 118.3, 124.3, 125.0, 126.9, 127.0, 128.0, 128.5, 128.7, 131.4, 136.5, 142.3, 154.5, 154.7, 155.7, 159.0; HRMS (ESI-TOF) *m/z* [M+H]⁺ calcd for C₂₄H₁₉O₃: 355.1329, Found: 355.1328.

4.3 Anti-*Trypanosoma cruzi* activity assay (Amastigotes and Trypomastigotes)

The *in vitro* anti-*T. cruzi* activity was evaluated on L929 cells (mouse fibroblasts) infected with Tulahuen strain of the parasite expressing the *Escherichia coli* β-galactosidase as reporter gene according to the method described previously^[25]. Briefly, for the bioassay, 4,000 L929 cells were added to each well of a 96-well microtiter plate. After an overnight incubation, 40,000 trypomastigotes were added to the cells and incubated for 2 h. Then the medium containing extracellular parasites was replaced with 200 μl of fresh medium and the plate was incubated for an additional 48 h to establish the infection. For IC₅₀ determination, the cells were exposed to each synthesized compound at serial decreasing dilutions and the plate was incubated for 96 h. After this period, 50 μl of 500 μM chlorophenol red beta-*D*-galactopyranoside (CPRG) in 0.5% Nonidet P40 was added to each well, and the plate was incubated for 16 to 20 h, after which the absorbance at 570 nm was measured. Controls with uninfected cells, untreated infected cells, infected cells treated with benznidazole at 3.8 μM (positive control) or DMSO 1% were used. The results were expressed as the percentage of *T. cruzi* growth inhibition in compound-tested cells as compared to the infected cells and untreated cells. The IC₅₀ values were calculated by linear interpolation. Quadruplicates were run in the same plate, and the experiments were repeated at least once.

4.4 Anti-*Trypanosoma cruzi* activity assay (Epimastigotes)

In this study, epimastigotes of the Y strain from *T. cruzi* were used. Epimastigotes obtained in exponential growth phase were washed with LIT medium 2 times in sterile PBS at pH 7.2 (1500 g) for 10 min at 4 °C. The number of parasites was determined in a Neubauer chamber. Next, the parasites were suspended in LIT medium, which was further supplemented with 10% FBS (Fetal Bovine Serum inactivated at 56 °C), and the concentration of epimastigotes adjusted to 5 × 10⁶ epimastigotes/mL. With the goal of

Accepted Article
screening samples with possible biological activity against *T. cruzi*, compounds were incubated in 48 well Nunc plates containing 800 μL of the suspension of parasites and 200 μL of the test compounds at different concentrations (40, 20, 10 and 1.6 $\mu\text{g}/\text{mL}$) diluted in sterile DMSO for 72 h in duplicate. As a negative control, the parasites were incubated in the absence of test compound and in the presence of 1% DMSO. Benznidazole (40, 20, 10 and 1.6 $\mu\text{g}/\text{mL}$) was used as positive control in tests against *T. cruzi*. The activity was determined by counting in a Neubauer chamber and subsequent statistical evaluation. The results are expressed as IC_{50} . The tests were repeated 2 times with the objective of evaluating the maintenance of the activity of the compounds and reproducibility of results.

4.5 *In vitro* cytotoxic test of trypanocidal compounds

The active compounds were tested *in vitro* for determination of cellular toxicity against uninfected L-929 cells using the alamarBlue® dye. The cells were exposed to compounds at increasing concentrations starting at IC_{50} value for *T. cruzi*. After 96 h of incubation with the tested compounds, the alamarBlue® was added and the absorbance at 570 and 600 nm measured after 4-6 h. The cell viability was expressed as the percentage of difference in the reduction between treated and untreated cells. IC_{50} values were calculated by linear interpolation and the selectivity index (SI) was determined based on the ratio of the IC_{50} value in the host cell divided by the IC_{50} value of the parasite. Quadruplicates were run in the same plate, and the experiments were repeated at least once.

4.6 Molecular Docking Studies

The enzyme from both organisms, *T. cruzi* and Human, including water of crystallization and ligands, was obtained from the “Protein Data Bank” (PDB). The codes are, respectively 1TCD and 4POC. Three-dimensional structures of the coumarins were obtained from Spartan Pro. The compounds were docked in the active sites using Molegro Virtual Docker 2006 (Thomsen and Christensen, 2006), which predicts the most likely conformation that a ligand will adopt for binding to a macromolecule.

Acknowledgements

This work was supported by the Brazilian funding agency Fundação de Amparo à Pesquisa do Estado de Minas Gerais (FAPEMIG) under research grant project code APQ-01629-16. This study was financed in part by the Coordenação de Aperfeiçoamento de Pessoal de Nível Superior - Brasil (CAPES) - Finance Code 001. Authors gratefully acknowledge the generous financial support from the Universidade Federal de Ouro Preto (UFOP), FAPEMIG and the Conselho Nacional de Desenvolvimento Científico e Tecnológico (CNPq). The authors thank the Program for Technological Development of Tools for Health-PDTIS-FIOCRUZ for use of its facilities. The authors would also like to thank Prof. Dr. Robson Jose de Cassia Afonso (UFOP) and Ananda Lima Sanson (UFOP) for the excellent mass spectroemtry service. Policarpo Ademar Sales Junior is research fellow supported by Programa de Pós-graduação em Ciências da Saúde, Fiocruz Minas (CAPES/PNPD).

List of the figure legends

Figure 1: Coumarin and isocoumarin natural products with *in vitro* activity against *T. cruzi*.

Figure 2: Synthetic coumarin compounds with *in vitro* activity against *T. cruzi*.

Scheme 1: Synthesis of tricyclic coumarins **3a-r**.

Figure 3: Chiral catalyst **4**.

Figure 4: - π stacking interaction between the compound (**3p**) and amino acid residues Tyr103.

Figure 5: Interactions between the compound (**3e**) (red) and TIM *T. cruzi* enzyme.

Figure 6: Overlap of the conformations adopted by the compounds **3e** and **3p** in the active site of *T. cruzi* TIM enzyme.

Figure 7: View of intramolecular π stacking interactions for compounds **3m** (pink) and **3k** (blue)

Figure 8: (a) Hydrogen and π stacking interactions of the compound **3r**; (b) more stable conformation adopted by compound **3r** in *T. cruzi* TIM enzyme.

Table 1 - Interaction energy values for enzyme-ligand complex (kcal mol⁻¹).

Table 2 - *In vitro* trypanocidal activity, cytotoxicity, selectivity index and physicochemical properties of bioactive tricyclic coumarins.

Conflicts of interest: There are no conflicts of interest to declare.

References

- [1] A. M. Argolo, M. Felix, R. Pacheco, J. Costa, *SciELO Books*. **2008**, 63-63.
- [2] J. R. Coura, S. L. Castro, *Mem Inst Oswaldo Cruz*. **2002**, *97(1)*,3-24.
- [3] World Health Organization (WHO). **2015**, *3*, 191-191.
- [4] World Health Organization (WHO), Chagas disease: [http://www.who.int/news-room/fact-sheets/detail/chagas-disease-\(american-trypanosomiasis\)](http://www.who.int/news-room/fact-sheets/detail/chagas-disease-(american-trypanosomiasis)) (accessed, July 2017).
- [5] G. A. Schmunis, *Mem Inst Oswaldo Cruz*. **2007**, *102*, 75-86.
- [6] F. M. Oliveira, A. T. Nagao-Dias, V. M. O. Pontes, de Souza Júnior A. S., H. L. Coelho, I. C. B. Coelho, *Revista de Patologia Tropical*. **2008**, *37*, 209-228.
- [7] P. A. S. Junior, I. Molina, S. M. F. Murta, A. Sánchez-Montalvá, F. Salvador, R. C. Oliveira, C. M. Carneiro, *rev. Am J Trop Med Hyg*. **2017**, *97*, 1289-1303.
- [8] K. N. Venugopala, V. Rashmi, B. Odhav, *Biomed Res Int*. **2013**, 2013.
- [9] T. M. Costa, L. B. B. Tavares, D. Oliveira, *Appl Microbiol Biotechnol*. **2016**, *100*, 6571-6584.
- [10] M. Steffensky, A. Mühlenweg, Z. X. Wang, S. M. Li, L. Heide, *Antimicrob Agents Chemother*. **2000**, *44*, 1214-1222.
- [11] A. Rea, A. G. Tempone, E. G. Pinto, J. T. Mesquita, E. Rodrigues, L. G. M. Silva, J. H. G. Lago, *PLoS neglected tropical diseases*. **2013**, *7*, e2556.
- [12] F. Pavao, M. S. Castilho, M. T. Pupo, R. L. A. Dias, A. G. Correa, J. B. Fernandes, G. Oliva, *FEBS lett*. **2002**, *520*, 13-17.
- [13] J. Gayosso-De-Lucio, M. Torres-Valencia, A. Rojo-Domínguez, H. Nájera-Peña, B. Aguirre-López, J. Salas-Pacheco, A. Téllez-Valencia, *Bioorganic Med. Chem. Lett*. **2009**, *19*, 5936-5939.
- [14] A. Muñoz, A. Fonseca, M. J. Matos, E. Uriarte, L. Santana, F. Borges, C. Olea-Azar *ChemistrySelect*. **2016**; *1*, 4957-4964.
- [15] S. Vazquez-Rodriguez, R. F. Guinez, M. J. Matos, C. Olea-Azar, J. D. Maya, E. Uriarte, L. Santana, *Med Chem*. **2016**, *12*, 537-543.
- [16] N. Robledo-O’Ryan, M. J. Matos, S. Vazquez-Rodriguez, L. Santana, E. Uriarte, M. Moncada-Basuato, C. Olea-Azar, *Bioorganic Med. Chem*. **2017**, *25*, 621-632.
- [17] K. E. Ozboya, T. Rovis, *Chem Sci*. **2011**, *2*, 1835-1838.

- [18] D. M. Flanigan, F. Romanov-Michailidis, N. A. White, T. Rovis, *Chem Rev.* **2015**, *115*, 9307-9387.
- [19] J. R. Alaniz, M. S. Kerr, J. L. Moore, T. Rovis, *Org. Chem.* **2008**, *73*, 2033-2040.
- [20] S. C. Cullen, T. Rovis, *Org Lett.* **2008**, *10*, 3141-3144.
- [21] J. C. L. Menezes, L. B. A. Vaz, P. M. de Abreu Vieira, K. da Silva Fonseca, C. M. Carneiro, J. G. Taylor. *Molecules.* **2014**, *20*, 43-51.
- [22] D. R. M. Moreira, A. C. Lima Leite, M. V. O. Cardoso, R. M. Srivastava, M. Z. Hernandez, M. M. Rabello, E. T. Guimaraes, *ChemMedChem.* **2014**, *9*, 177-188.
- [23] P. R. Elias, G. S. Coelho, V. F. Xavier, P. A. Sales Junior, A. J. Romanha, S. M. F. Murta, C. M. Carneiro, J. G. Taylor. *Molecules.* **2016**, *21(10)*, 1342.
- [24] A. A. de Souza, V. F. Xavier, G. S. Coelho, P. A. Sales Junior, A. J. Romanha, S. M. F. Murta, C. M. Carneiro, J. G. Taylor. *J. Braz. Chem. Soc.* **2018**, *29(2)*, 269-277.
- [25] A. J. Romanha, S. L. Castro, M. D. Soeiro, J. Lannes-Vieira, I. Ribeiro, A. Talvani, B. Bourdin, B. Blum, B. Oliveira, C. Zani, C. Spadafora, *Mem Inst Oswaldo Cruz.* **2010**, *105*, 233-238.
- [26] A. M. A. Velasquez, A. I. Francisco, A. A. N. Kohatsu, F. A. D. J. Silva, D. F. Rodrigues, R. G. D. S. Teixeira, B. G. Chiari, M. G. J. Almeida, V. L. B. Isaac, M. D. Varga, R. M. B. Cicarelli, *Bioorganic Med. Chem. Lett.* **2014**, *24*, 1707-1710.
- [27] M. B. Soares, J. F. O. Costa, M. Santos de Sá, R. Ribeiro dos Santos, P. Pigeon, G. Jaouen, A. E. G. Santana, M. O. F. Goulart, E. Hillard, *Drug Dev Res.* **2010**, *71*, 69-75.
- [28] J. A. Urbina, R. Lira, G. Visbal, J. Bartrolí, *Antimicrob Agents Chemother.* **2000**, *44*, 2498-2502.
- [29] J. A. Urbina, G. Payares, C. Sanoja, R. Lira, A. J. Romanha, *Int J Antimicrob Agents*, **2003**, *21*, 27-38.
- [30] C. A. Lipinski, F. Lombardo, B. W. Dominy, P. J. Feeney, *Adv Drug Deliv Ver.* **1997**, *23*, 3-25.

Table 1 - Interaction energy values for enzyme-ligand complex (kcal mol⁻¹).

Compound	Human TIM (Enzyme 4POC)		<i>T. cruzi</i> TIM (Enzyme 1TCD)	
	Interaction energy (kcal mol ⁻¹)	Amino acid residues	Interaction energy (kcal mol ⁻¹)	Amino acid residues
(3a)	-141.09	Asn65 Arg98	-133.62	-
(3b)	-56.11	Arg98	-113.15	-
(3c)	-45.53	Arg98	-126.41	-
(3d)	-109.44	Asn65	-135.63	-
(3e)	-109.80	Asn65 Arg98	-139.35	Arg99
(3f)	-86.92	Arg98	-116.38	-
(3g)	-144.60	Asn65 Arg98	-118.70	-
(3h)	-150.79	Asn65 Arg98	-129.77	-
(3i)	-121.06	Asn65 Arg98 Ile78	-129.77	-
(3j)	-74.83	Asn65 Arg98	-132.24	Arg99
(3k)	-74.83	Asn65 Gly76 Gly112	-76.47	Arg99
(3l)	-78.72	Asn65 Thr45	-63.65	-
(3m)	-80.33	Asn65	-83.68	Lys113
(3n)	-30.75	Asn65 Arg98	-121.22	-
(3p)	-110.14	Asn65	-143.12	-
(3q)	-47.49	Arg98 Thr45	-92.47	-
(3r)	-134.31	Asn65 Arg98 Ile78 Tyr67	-137.75	Glu78 Arg99

Table 2 - *In vitro* trypanocidal activity, cytotoxicity, selectivity index and physicochemical properties of bioactive tricyclic coumarins.

Compound	<i>In vitro</i> Activity			Lipinski's rule of five					TPSA (Å ²)	Volume Å ³	NRB	Risk Toxicity			
	Trypanocide IC ₅₀ (μM) ± 0.2	Cytotoxicity CC ₅₀ (μM) ± 2.0	SI	HBA	HBD	MW (g.mol ⁻¹)	logP	Violations				M	T	I	RE
3a	2.5	320	128	2	0	338.13	5.54	1	30.21	311.02	2	NR	NR	NR	LR
3b	2.4	160	66	2	0	372.09	6.17	1	30.21	324.56	2	NR	NR	NR	LR
3c	6.1	160	26	3	0	368.14	5.58	1	39.45	336.56	3	NR	NR	NR	LR
3d	Inactive	320	-	2	0	416.04	6.33	1	30.21	328.90	2	NR	NR	NR	LR
3e	0.6	160	262	3	0	368.14	5.60	1	39.45	336.56	3	NR	NR	NR	LR
3f	1.4	40	28	2	0	356.12	5.71	1	30.21	315.95	2	NR	NR	NR	LR
3g	3.4	80	23	2	0	372.09	6.20	1	30.21	324.56	2	NR	NR	NR	LR
3h	Inactive	250	-	2	0	406.05	6.87	1	30.21	338.09	2	NR	NR	NR	LR
3i	3.1	160	51	3	0	402.10	6.25	1	39.45	350.10	3	NR	NR	NR	LR
3j	2.6	294	13	4	0	358.12	4.36	0	52.59	318.13	3	NR	NR	NR	NR
3k	9.3	80	9	3	0	341.14	4.29	0	35.15	312.95	2	NR	NR	NR	NR
3l	0.6	40	64	3	0	402.10	5.76	1	39.45	350.10	3	NR	NR	NR	LR
3m	80.0	320	4	3	0	328.11	4.33	0	43.35	292.59	2	NR	NR	NR	NR
3n	67.0	80	1	4	0	340.12	2.73	0	55.99	302.71	2	NR	NR	NR	NR
3o	2.4	320	33	2	0	446.09	4.02	0	30.21	394.80	4	HR	LR	NR	LR
3p	0.4	39	83	2	0	364.14	6.20	1	30.21	338.44	3	NR	NR	NR	NR
3q	81.0	350	4	3	0	444.17	7.19	1	39.45	408.21	5	NR	NR	NR	LR
3r	4.2	20	5	3	1	354.12	5.06	1	50.44	319.04	2	NR	NR	NR	LR
Bz	3.8	2381	625	-	-	-	-	-	-	-	-	-	-	-	-

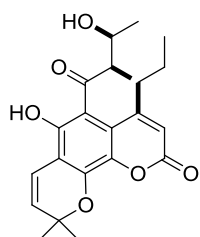
IC₅₀: 50% inhibitory concentration. CC₅₀: 50% cytotoxic concentration determined using mammalian L929 cells.

SI: selectivity index calculated from CC₅₀/IC₅₀. LogP: octanol/water partition coefficient, TPSA: total polar surface area, HBA = hydrogen bond acceptors, HBD = hydrogen bond donors, NRB = number of rotatable bonds, M = mutagenicity, T = tumorigenicity, I = skin irritation, RE = reproductive effect, NR = no risk, LR = low risk, MR = medium risk, HR = high risk



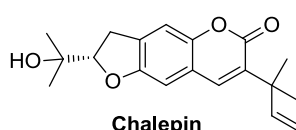
Mammea B/BA

IC₅₀ (epimastigote) = 15 μM.
 IC₅₀ (trypomastigote) = 25 μM.
 IC₅₀ (cytotoxicity) = 223 μM.



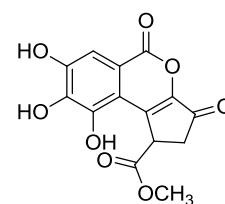
Soulamarin

IC₅₀ (amastigote) = 210 μM.
 IC₅₀ (trypomastigote) = 219 μM.
 IC₅₀ (cytotoxicity) = 278 μM.



Chalepin

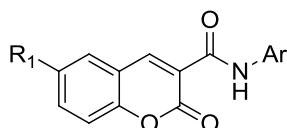
IC₅₀ (GAPDH enzyme) = 64 μM.



**Brevifolin
 carboxylate derivative**

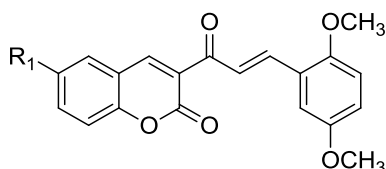
IC₅₀ (TcTIM) = 6.5 μM.
 IC₅₀ (hTIM) = <1 μM.

Figure 1: Coumarin and isocoumarin natural products with *in vitro* activity against *T. cruzi*.



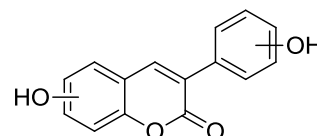
3-Carboxamidocoumarins

IC₅₀ (epimastigote) = 20 - 82 μM.
 IC₅₀ (cytotoxicity) = 51 - 192 μM.



Coumarin - chalcone Hybrid

IC₅₀ (amastigote) = 2.9 μM.
 IC₅₀ (trypomastigote) = 2.6 μM.
 IC₅₀ (epimastigote) = 46.8 μM.
 IC₅₀ (cytotoxicity) = 6.1 μM.



3-Arylcoumarins

IC₅₀ (epimastigote) = 1.3 - 84.3 μM.
 IC₅₀ (cytotoxicity) = 26.1 - 397.6 μM.

Figure 2: Synthetic coumarin compounds with *in vitro* activity against *T. cruzi*.

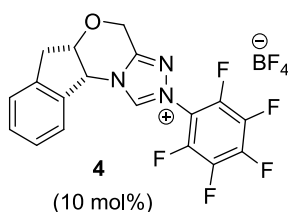


Figure 3: Chiral catalyst **4**.

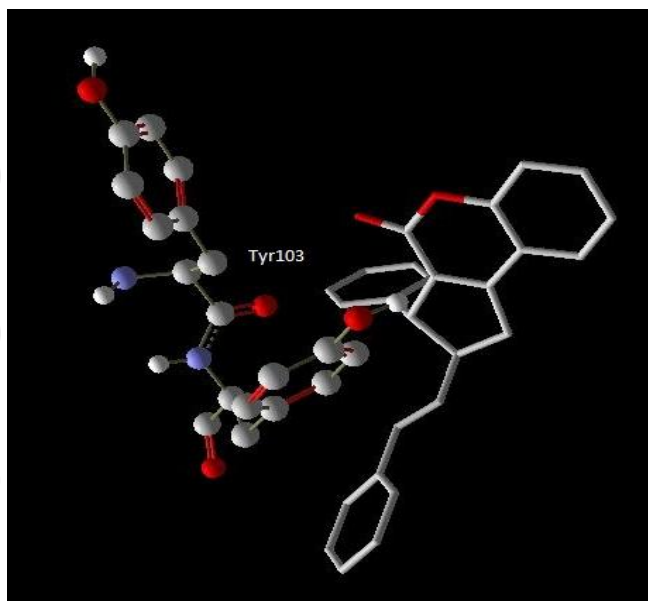


Figure 4: - π stacking interaction between the compound (**3p**) and amino acid residues Tyr103.

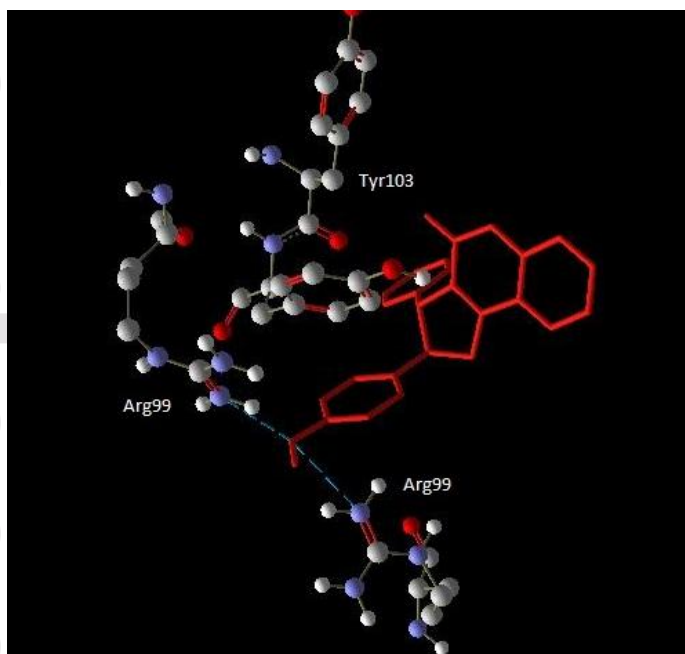


Figure 5: Interactions between the compound (**3e**) (red) and TIM *T. cruzi* enzyme.

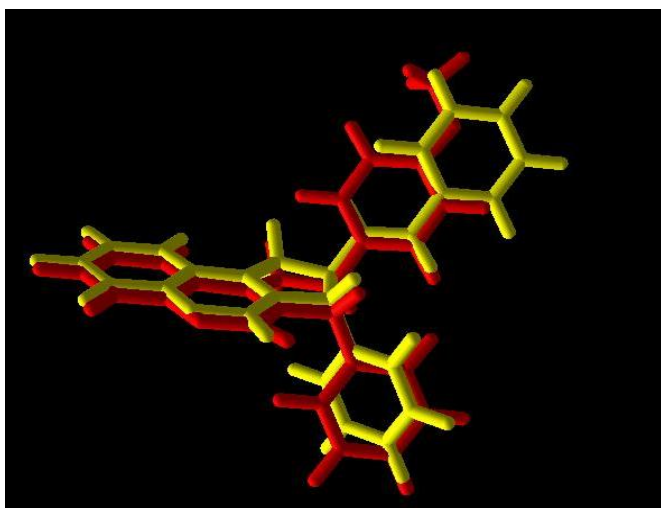


Figure 6: Overlap of the conformations adopted by the compounds **3e** and **3p** in the active site of *T. cruzi* TIM enzyme.

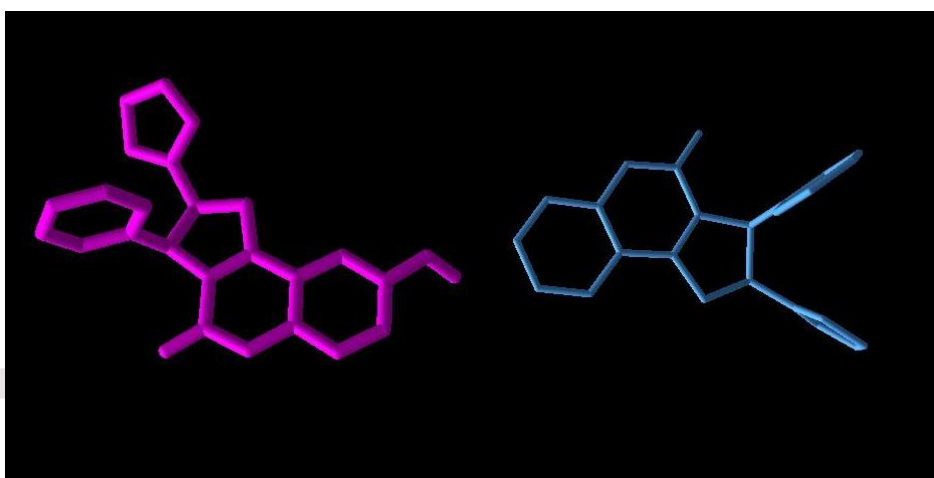


Figure 7: View of intramolecular π stacking interactions for compounds **3m** (pink) and **3k** (blue)

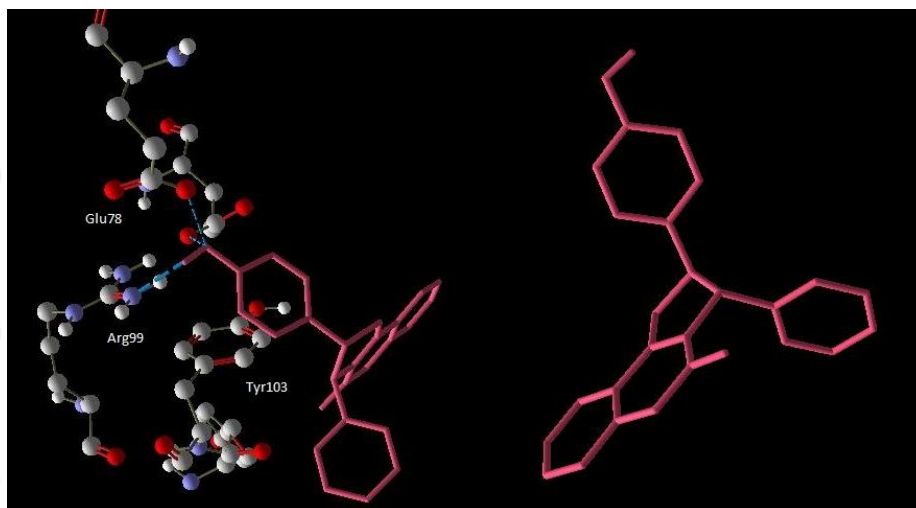
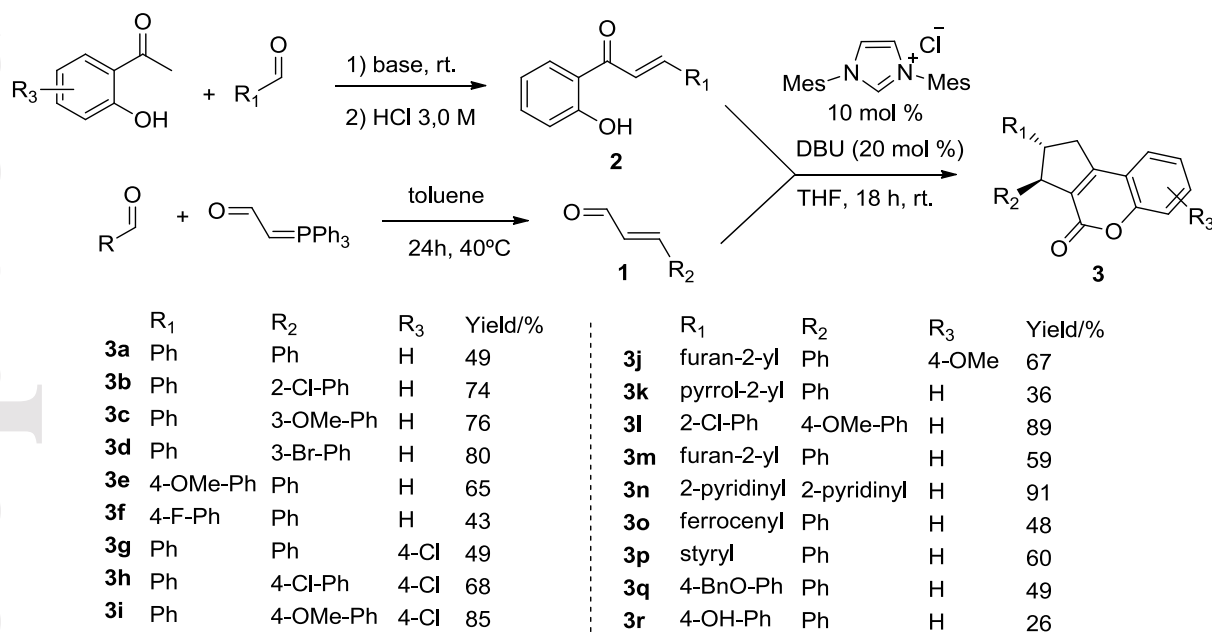


Figure 8: (a) Hydrogen and π stacking interactions of the compound **3r**; (b) more stable conformation adopted by compound **3r** in *T. cruzi* TIM enzyme.



Scheme 1: Synthesis of tricyclic coumarins **3a-r**